Cytometry Part B (Clinical Cytometry) 84B:71–81 (2013)

Original Article

A Systematic Analysis of Bone Marrow Cells by Flow Cytometry Defines a Specific Phenotypic Profile Beyond GPI Deficiency in Paroxysmal Nocturnal Hemoglobinuria

Francesco Mannelli,[1,2]* Sara Bencini,[1,2] Benedetta Peruzzi,[3] Ilaria Cutini,[1,2] Alessandro Sanna,[1,2] Matteo Benelli,[4] Alberto Magi,[5] Giacomo Gianfaldoni,[1,2] Giada Rotunno,[1,2] Valentina Carrai,[1,2] Anna Maria Grazia Gelli,[3] Veronica Valle,[6] Valeria Santini,[1,2] Rosario Notaro,[2] Lucio Luzzatto,[2] and Alberto Bosi[1,2]

[1]Unità Funzionale di Ematologia, Università degli Studi, AOU Careggi, Florence, Italy

[2]Istituto Toscano Tumori, Florence, Italy

[3]SOD Laboratorio Centrale, Settore Citometria Clinica, AOU Careggi, Florence, Italy

[4]SOD Diagnostica Genetica, AOU Careggi, Florence, Italy

[5]Facoltà di Medicina, Università degli Studi di Firenze, Florence, Italy

[6]Unità di Ematologia, Dipartimento "Biotecnologie Cellulari ed Ematologia", Università Sapienza, Rome, Italy

Background. Paroxysmal nocturnal hemoglobinuria (PNH) is a unique disorder caused by a PIG-A gene mutation in a stem cell clone. Its clinical picture can sometimes make challenging the distinction from other disorders, and especially from myelodysplastic syndromes (MDS), since both diseases correlate with cytopenias and morphological abnormalities of bone marrow (BM) cells. Recently, flow cytometry (FC) has been proposed to integrate the morphologic assessment of BM dysplasia, and thus to improve the diagnostics of MDS.

Methods. In the present study, we have analyzed systematically FC data resulting from the study of BM cells from patients with PNH and MDS.

Results. Our data demonstrated abnormalities in PNH beyond the deficiency of glycosylphosphatidylinositol-linked proteins and the application of a systematic approach allowed us to separate effectively MDS and PNH in a cluster analysis and to highlight disease-specific abnormalities. Indeed, the parallel evaluation of some key parameters, *i.e.* patterns of expression of CD45 and CD10, provided information with practical diagnostic usefulness in the distinction between PNH and MDS. Moreover, the hypo-expression of CD36 that we observed on monocytes might be related to the thrombotic tendency in PNH.

Conclusions. We investigated systematically the phenotypic profile of BM cells from patients with PNH; our data provide useful antigenic patterns to solve between PNH and MDS, sometimes morphologically overlapping. Moreover, some PNH-related phenotypic changes might be involved in the physiopathology of the disease and further studies addressing this issue are warranted. © **2012 International Clinical Cytometry Society**

Key terms: paroxysmal nocturnal hemoglobinuria; myelodysplastic syndromes; flow cytometry; phenotypic score; cluster analysis

How to cite this article: Mannelli F, Bencini S, Cutini, I, Sanna A, Benelli M, Magi A, Gianfaldoni G, Rotunno G, Carrai V, Gelli AMG, Valle V, Santini V, Notaro R, Luzzatto L, Alberto B. A systematic analysis of bone marrow cells by flow cytometry defines a specific phenotypic profile beyond GPI deficiency in paroxysmal nocturnal hemoglobinuria. Cytometry Part B 2013; 84B: 71–81.

Additional Supporting Information may be found in the online version of this article.

*Correspondence to: Francesco Mannelli, UF di Ematologia, Dipartimento di Area Critica Medico-Chirurgica, Università di Firenze, and Istituto Toscano Tumori, Largo Brambilla 3, 50134 Florence, Italy.

E-mail: francesco.mannelli@unifi.it; http://www.ematologiafirenze.com.

Received 9 May 2012; Revision 26 November 2012; Accepted 27 November 2012

Published online 26 December 2012 in Wiley Online Library (wileyonlinelibrary.com).

DOI: 10.1002/cyto.b.21064

Paroxysmal nocturnal hemoglobinuria (PNH) is a unique disorder caused by a PIG-A gene mutation in a stem cell clone [1,2]. As a consequence, blood cells completely or partially lack surface proteins that are tethered to the membrane through the glycosylphosphatidylinositol (GPI) anchor [3,4]. The resulting absence of CD55 and CD59 molecules on red cells renders them sensitive to complement-mediated intravascular hemolysis and associated hemoglobinuria [5]. PNH often shows a component of bone marrow (BM) failure, which sometimes determines pancytopenia. This clinical picture can make it challenging to distinguish PNH from other cytopenia-causing disorders, and especially from myelodysplastic syndromes (MDS). There are pathophysiological links between MDS and PNH and PNH clones can be detected in a relevant fraction of MDS patients. The presence of such small populations of GPI-deficient cells correlates with important prognostic and therapeutic implications in the setting of MDS. The International PNH Group has, therefore, defined these conditions as subclinical PNH [6].

The diagnosis of PNH and its distinction from MDS strictly rely on a specific clinical suspicion, which drives the application of diagnostic techniques and interpretation of the results. Indeed, morphology still represents the cornerstone for the diagnosis of MDS: dysplastic features in a significant fraction of BM cells provide evidence of ineffective hemopoiesis, which is the common denominator of this heterogeneous group of disorders [7]. However, morphological abnormalities overlapping with those observed in MDS have been described in PNH and are considered part of the *spectrum* of its hematological picture [8]. It is important to note that not even an abnormal karyotype can rule out a diagnosis of PNH, since abnormalities have been reported in up to 24% of patients [8].

Flow cytometry (FC) is established as the method of choice for diagnosing PNH [9,10]; nevertheless, a specific analysis aiming at this depends on the clinical suspicion. In fact, it includes the study of GPI-related molecules on red cells and it is performed on peripheral blood (PB), whose analysis is less prone to be misinterpreted than on BM, due to the dependency on maturation of some GPI-related antigens. Many reports have proposed FC as a useful technique in the diagnosis of MDS, mainly by investigating the expression of key antigens during maturation [11–15]. Such an approach on BM samples in view of cytopenia may not be able to distinguish PNH from MDS. On the other hand, the progressive role of FC as a reliable technique to investigate dysplasia gives the opportunity to get an insight into PNH phenotype, beyond GPI-dependent abnormalities. In the present study, we have carried out a systematic analysis of BM samples from patients with PNH and MDS; our aim was to compare the whole BM phenotypic profile in order to pinpoint distinctive patterns associated with these diseases.

MATERIALS AND METHODS

Patients, Controls, and Samples

Patients with untreated PNH (n=8) and MDS (n=30) were included in the study. BM samples were sent to our laboratory in view of cytopenia to address the suspicion of MDS. On the basis of a parallel analysis on PB (see below), when clinically required, some patients were eventually demonstrated to have PNH. MDS cases were classified according to WHO [7]. BM samples from 21 healthy donors and patients with lymphoma at staging without BM involvement were included as controls. Some patients with vitamin B12 deficiency (B12 def) were studied by the same approach as a "positive" control (morphologic dysplasia due to a different cause). All samples were fresh and anti-coagulated with EDTA. The study was approved by an institutional review board, and the patients were enrolled after obtaining a written informed consent from them in accordance with the Declaration of Helsinki.

Morphologic Analysis

For MDS diagnosis, according to WHO [7], at least 10% of the cells of at least one myeloid BM lineage (erythroid, granulocytic, megakaryocytic) had to show unequivocal dysplasia on May–Grunwald–Giemsa-stained BM aspirates.

Karyotyping and IPSS Assessment

Cytogenetic analysis was performed on BM cells at diagnosis according to the International System for Human Cytogenetic Nomenclature [16]. International prognostic scoring system was assessed according to published evidences [17].

BM FC Analysis

Cells, 2 x 10^6 of a fresh BM suspension, were stained for surface markers using a stain-lyse-and-then-wash procedure; intracellular nuclear and cytoplasmic staining were performed after cell fixation and permeabilization, using the Fix and Perm reagent kit (Invitrogen, Carlsbad, CA, USA). The following combinations of monoclonal antibodies (MoAb) in four-color staining (fluorescein isothiocyanate/phycoerythrin/peridinin chlorophyll protein/allophycocyanin) were used:

HLA-DR/CD117/CD45/CD34; HLA-DR/CD123/CD45/CD34; CD11b/CD13/CD45/CD34; CD22/CD33/CD45/CD34; CD15/CD16/CD45/CD34; CD71/CD105/CD45/CD34; CD2/CD56/CD45/CD34; CD65/NG2/CD45/CD34; CD36/CD64/CD45/CD34; CD14/CD64/CD45/CD34; CD34/CD203c/CD45/CD38; nTdT/cyMPO/CD45/CD34; CD19/cyCD79a/CD45/CD34; cyCD3/CD7/CD45/CD34.

Clones of MoAbs were as follows: HLA-DR: G46-6; CD117: YB5.B8; CD45: HI30; CD34: 581; CD123: 7G3; CD11b: M1/70; CD13: WM15; CD22: S-HCL-1; CD33: HIM3-4; CD15: HI98; CD16: 3G8; CD71: M-A712; CD105: SN6; CD2: RPA-2.10; CD56: MY31; CD65: 88H7; NG2: 7.1; CD36: CB38; CD64: 10.1; CD14: M5E2; CD203c: 97A6; CD38: HB7; nTdT: HT-6; cyMPO: MPO-7; CD19: 4G7; cyCD79a: HM-57; cyCD3: HIT3a; CD7: M-T701.

All MoAbs were purchased from Becton Dickinson (BD,San Jose, CA, USA), excluding nTdT, cyMPO (Dako, Glostrup, Denmark), CD11b, CD65, CD203c (Immunotech, Marseille, France), and CD105 (e-Bioscience, San

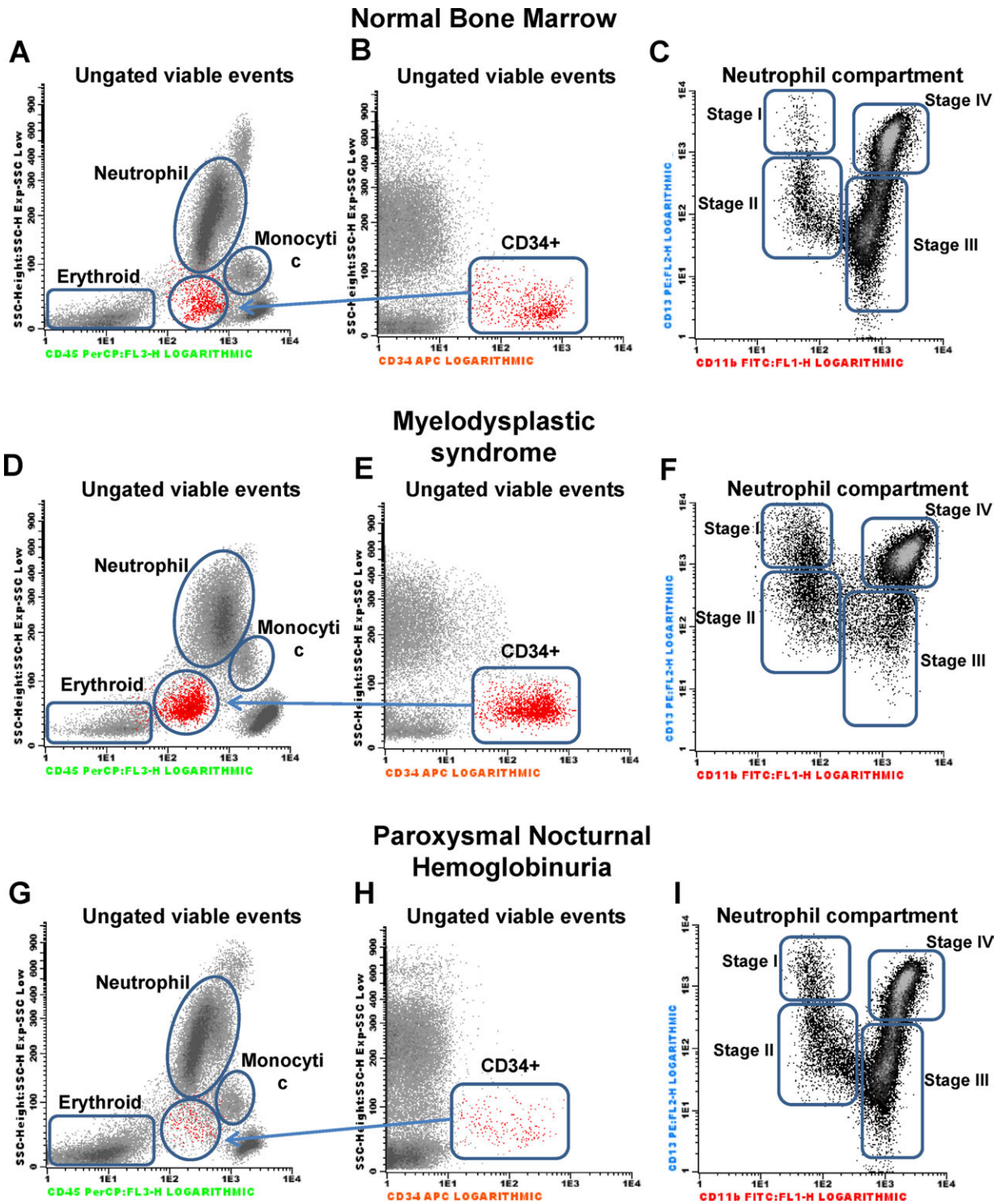

FIG. 1. Multiple abnormalities detected by flow cytometry in the bone marrow cells of MDS and PNH patients: illustrated examples. Bivariate dot plots illustrating how the different cell compartments were identified on the basis of light scatter characteristics and reactivity for CD45 PerCP and CD34 APC (**A**,**B**,**D**,**E**,**G**,**H**). Identification of the different subsets within neutrophil compartment on the basis of the combined expression of CD13 and CD11b (**C**,**F**,**I**). Dot plots were created by using Infinicyt software. [Color figure can be viewed in the online issue which is available at wileyonlinelibrary.com]

Diego, CA, USA). Data acquisition was performed using a FACSCalibur flow cytometer (BD) and Cell Quest Pro software (BD). A total of 50,000 events of BM cellularity *per* tube was acquired; if required, a second step was performed in order to collect at least 1 x 10^3 CD34+ cells through an electronic gate. For data analysis,

Table 1
Characteristics of Patients with PNH

Pt	Age/gender	WBC ($x10^9$/L)	Hb (g/dL)	MCV (fL)	Plt ($x\ 10^9$/L)	LDH (U/L)	PNH RBC (CD59-neg)	PNH PMN (CD66b-neg)	PNH mono (CD14-neg)
1	35/M	3.92	10.9	87	129	980	11.3%	80.5%	79.7%
2	73/M	4.0	12.5	104	136	936	36.3%	56.0%	54.4%
3	59/F	4.7	9.3	109	122	1211	37.4%	70.6%	80.3%
4	80/M	7.4	9.9	109	292	447	18.5%	60.4%	63.4%
5	61/F	4.1	8.3	111	21	784	37.0%	76.0%	87.0%
6	62/M	2.9	8.7	104	105	1479	12.0%	91.0%	95.0%
7	28/M	2.4	6.9	96	46	327	17.0%	94.0%	89.0%
8	21/M	2.8	7.3	103	128	1447	15.6%	89.5%	90.4%

Abbreviations: PNH, paroxysmal nocturnal hemoglobinuria; LDH, lactate dehydrogenase; MCV, mean corpuscular volume; PMN, poly-morpho-nuclear; RBC, red blood cells.

Infinicyt (Cytognos SL, Salamanca, Spain) software was used. Our approach was adapted from the one described by Matarraz et al. [13]. Briefly, some major BM cell compartments were identified on the basis of forward (FSC) and sideward (SSC) light scatter characteristics and their reactivity for CD45 and CD34 (Figs 1A,B,D,E,G,H). These subsets were (i) myeloid CD34+/nTdT-/CD117+ fraction of CD34+ cells; (ii) CD34+ B-cell precursors, featured by HLA-DRhi/CyMPO-/nTdT+/CD117- profile with low SSC; (iii) maturing granulocytic compartment, selected on the basis of CD45+dim/CD34- with high SSC, within which four maturation stages were identified depending on reactivity for CD13 and CD11b (Fig. 1 C,F,I); (iv) mature monocytic compartment (CD45+hi/CD34- with intermediate SSC signal); and (v) mature erythroid compartment (CD45-/CD34- with low SSC). A series of 69 phenotypic parameters were defined (17 for CD34+, 27 for neutrophil, 15 for monocytic, and 10 for erythroid compartment) and expressed as percentage of positive cells for a given antigen within a cell compartment and/or its mean fluorescence intensity (MFI; arbitrary relative linear units, scaled from 0 to 10^4). Normal phenotypic profile was defined on normal BM samples as the interval between mean value $\pm$ two standard deviations for each parameter. Phenotypic aberrancies in MDS, B12 def, and PNH were defined considering deviations from the normal profile. Daily instrument quality controls including fluorescence standardization, linearity assessment, and spectral compensation were performed to ensure identical operation from day to day according to published evidence [18,19]. Specifically, instrument setup, calibration, and quality control were checked during the study using commercial standard reagents (Spherocaliflow QC kit; Spherotec, Lybertyville, IL, USA).

PNH FC Analysis on PB

PNH diagnosis was performed by FC on PB as elsewhere described [9,20]. Data acquisition was carried out by a FACS Canto II (BD) flow cytometer; for data analysis, Diva Software (BD) was used. Analysis of red blood cells (RBC) was performed on 3 μl of PB diluted 1:200 with PBS; 50 μl of the diluted sample were incubated with anti-CD59 PE MoAb (Clone MEM43, Serotec) for 15 min in the dark at room temperature and washed twice with PBS. A total of 20,000 events of PB cellularity *per* tube was acquired. Analysis of white blood cells (WBC) was performed on 60 μl of PB incubated with a combination of CD66b FITC, CD33 PE, CD45 PerCP-Cy5.5, and CD14 APC MoAbs (all purchased from BD) for 15 min in the dark at room temperature. After incubation, the samples were incubated with an erythrocyte-lysing reagent (2 ml), then washed twice with PBS. A total of 20,000 events of CD45-positive cells *per* tube was acquired. Neutrophils and monocytes were identified on the basis of CD45 vs SSC dot plot as a first step, and further purified through CD33 expression intensity as a second step. GPI-deficient cells were defined by negativity for CD66b on neutrophils, CD14 on monocytes, and CD59 on RBC.

Statistical Analysis

Data were processed using GraphPad InStat (GraphPad Software, San Diego, CA USA) and SPSS (Statsoft Inc, Tulsa, OK, USA) software. Comparisons between two or more groups were performed using Mann–Whitney U test. P values <0.05 were considered to be associated with statistical significance. To test the capability of the parameters in segregating different diseases, we performed Ward's hierarchical clustering. Briefly, data were stored in a database system (Microsoft Excel; Microsoft, Seattle, WA, USA) and were normalized. In order to normalize the data of each individual, we calculated the mean value of each parameter across all normal BM samples. Normalized data were obtained by dividing the value of each individual by the calculated mean. Finally, all the data were log2-transformed and the resulting normalized log2 ratios were used for hierarchical clustering analyses (custom R scripts, http://cran.r-project.org).

RESULTS

Patients' Characteristics

From 2008 to 2011, BM samples from eight PNH patients were studied; their characteristics are summarized in Table 1. Five patients with B12 def were analyzed: B12 def was caused by nutritional deficiencies (two cases), absorption alteration due to gastrectomy (one case), and pernicious anemia (two cases). A total

Table 2
Phenotypic Characteristics of BM Cell Compartments

Phenotypic parameter	Controls (#21)	MDS (#30)	B12 def (#5)	PNH (#8)	p1	p2	p3
CD34+ compartment							
Total CD34+ %	1.0 ± 0.4	4.1 ± 4.1	1.3 ± 0.6	0.1 ± 0.1	0.003	ns	0.0006
B precursors	0.2 ± 0.2	0.04 ± 0.06	0.2 ± 0.2	0.02 ± 0.02	<0.0001	ns	0.0003
FSC MI	421 ± 42	426 ± 115	469 ± 65	468 ± 35	ns	ns	ns
SSC MI	59 ± 6	62 ± 15	65 ± 12	67 ± 3	ns	ns	0.005
CD45 MFI	450 ± 75	366 ± 174	415 ± 35	409 ± 102	0.0006	ns	ns
CD34 MFI	277 ± 98	340 ± 178	253 ± 73	230 ± 110	ns	0.003	ns
CD13 MFI	603 ± 169	616 ± 347	452 ± 206	650 ± 208	ns	ns	ns
CD33 MFI	380 ± 136	358 ± 253	222 ± 60	460 ± 188	ns	ns	ns
CD117 MFI	613 ± 127	828 ± 457	600 ± 413	436 ± 101	ns	ns	0.003
HLA-DR MFI	1591 ± 356	1596 ± 1083	1325 ± 685	1438 ± 465	ns	ns	ns
CD7 %	14 ± 2.7	21 ± 17	16 ± 3	27 ± 11	ns	ns	0.0001
MPO %	34 ± 5	23 ± 11	30 ± 9	35 ± 5	0.0003	ns	ns
CD15 %	22 ± 4	22 ± 13	21 ± 7	27 ± 8	ns	ns	0.01
CD65 %	22 ± 6	15 ± 7	17 ± 5	16 ± 4	0.0002	0.02	ns
CD11b %	1.6 ± 1.6	5 ± 8	2.8 ± 1.3	1.5 ± 1.8	ns	ns	ns
CD38 %	90 ± 4	82 ± 17	86 ± 5	95 ± 5	ns	ns	0.02
CD25%	3 ± 1.6	8 ± 10	2 ± 2.2	2 ± 1.5	ns	ns	ns
Neutrophil compartment							
Total neutrophil %	64 ± 7	47 ± 18	47 ± 18	52 ± 13	0.0002	0.004	0.008
FSC MI	662 ± 40	637 ± 120	745 ± 109	632 ± 75	ns	ns	ns
SSC MI	226 ± 23	212 ± 37	291 ± 45	235 ± 30	ns	.002	ns
CD45 MFI	734 ± 151	611 ± 209	661 ± 69	681 ± 183	0.01	ns	ns
CD15 MFI	6426 ± 1090	6475 ± 1965	6976 ± 2691	6377 ± 1507	ns	ns	ns
CD15 CV	26.1 ± 11.5	32.5 ± 16.5	29.9 ± 18.5	30.0 ± 10.0	ns	ns	ns
CD16 %	52 ± 11	46 ± 19	36 ± 15	18 ± 11	ns	0.03	0.0001
CD13 MFI	910 ± 200	789 ± 466	393 ± 160	696 ± 245	ns	0.0001	ns
CD11b MFI	959 ± 155	1022 ± 504	1221 ± 962	914 ± 186	ns	ns	ns
CD65 MFI	1542 ± 481	1816 ± 792	1848 ± 735	1308 ± 420	ns	ns	ns
CD33 MFI	251 ± 111	363 ± 288	283 ± 74	136 ± 68	ns	ns	ns
CD64 MFI	266 ± 94	252 ± 214	324 ± 150	214 ± 145	ns	ns	ns
CD10 %	49 ± 13	42 ± 16	30 ± 10	60 ± 19	ns	0.009	ns
CD123 %	4.8 ± 7	8 ± 8	20 ± 17	3.1 ± 4.0	ns	0.04	ns
CD4 %	16 ± 6	29 ± 24	24 ± 5	11.5 ± 6.6	0.03	ns	ns
Stage I %	0.7 ± 0.5	2.4 ± 2.7	2.3 ± 1.5	1.0 ± 0.8	0.0004	0.002	ns
Stage II %	9.8 ± 4.7	17.8 ± 16.7	18.4 ± 5.7	6.7 ± 5.5	0.04	0.003	ns
Stage III %	36.6 ± 7.3	29.8 ± 13.6	44.4 ± 5.5	30.0 ± 13.2	0.03	0.03	ns
Stage IV %	53 ± 10.7	50.1 ± 18.8	34.9 ± 12.5	62.5 ± 18.4	ns	0.003	ns
Stage I FSC MI	681 ± 78	621 ± 125	705 ± 128	636 ± 65	ns	ns	ns
Stage II FSC MI	854 ± 69	728 ± 150	808 ± 82	742 ± 40	0.002	ns	0.002
Stage III FSC MI	716 ± 63	655 ± 132	756 ± 138	644 ± 65	ns	ns	0.008
Stage IV FSC MI	648 ± 57	608 ± 117	777 ± 141	580 ± 65	ns	ns	0.02
Stage I-III SSC MI	187 ± 23	193 ± 26	273 ± 49	201 ± 26	ns	0.0009	ns
Stage IV SSC MI	250 ± 31	228 ± 41	395 ± 34	250 ± 26	ns	<0.0001	ns
Stage I-III CD45	353 ± 111	441 ± 138	396 ± 63	321 ± 80	0.03	ns	ns
Stage IV CD45 MFI	702 ± 289	758 ± 259	638 ± 100	680 ± 264	ns	ns	ns
Monocytic compartment							
Total monocytic %	4.4 ± 0.95	5.8 ± 5.8	5.0 ± 3.7	4.0 ± 2.2	ns	ns	ns
FSC MI	462 ± 26	508 ± 79	560 ± 68	453 ± 45	0.02	0.0009	ns
SSC MI	98 ± 9	103 ± 15	101 ± 9	99 ± 13	ns	ns	ns
CD45 MFI	1810 ± 318	1638 ± 567	1650 ± 180	1619 ± 287	ns	0.002	ns
CD14 %	90 ± 4	81 ± 15	90 ± 6	25 ± 14	ns	ns	<0.0001
CD14 MFI	1367 ± 321	907 ± 550	1155 ± 292	384 ± 220	0.006	ns	<0.0001
CD45 MFI CD14neg	951 ± 110	918 ± 166	877 ± 80	1629 ± 143	ns	ns	<0.0001
CD45 MFI CD14pos	2088 ± 308	1743 ± 423	1896 ± 86	1752 ± 119	0.02	ns	ns
CD36 MFI	1245 ± 320	925 ± 514	1439 ± 1240	356 ± 156	0.003	ns	<0.0001
CD64 MFI	1681 ± 369	1885 ± 788	1585 ± 326	1392 ± 750	ns	ns	ns
CD13 MFI	1756 ± 718	1440 ± 997	1570 ± 1110	1540 ± 356	ns	ns	ns
CD11b MFI	1395 ± 290	1249 ± 714	1604 ± 1109	1308 ± 532	0.02	ns	ns
CD15 MFI	545 ± 186	1160 ± 1014	600 ± 330	817 ± 406	0.01	ns	ns
CD33 MFI	1085 ± 515	1445 ± 796	1000 ± 205	997 ± 437	ns	ns	ns
CD65 MFI	212 ± 143	351 ± 259	224 ± 61	152 ± 75	ns	ns	ns
Erythroid compartment							
Total erythroid %	9.9 ± 5.6	20.6 ± 13.3	30.3 ± 13.3	18.9 ± 14.4	0.002	<0.0001	ns
FSC MI	226 ± 14	258 ± 45	283 ± 28	238 ± 30	0.01	<0.0001	ns
SSC MI	20 ± 2.7	28 ± 9	30 ± 12	24 ± 5	<0.0001	0.002	0.03

Table 2
Phenotypic Characteristics of BM Cell Compartments (Continued)

Phenotypic parameter	Controls (#21)	MDS (#30)	B12 def (#5)	PNH (#8)	p1	p2	p3
CD45 MFI	7 ± 4	12 ± 11	19 ± 12	8.6 ± 4.3	0.01	0.004	ns
CD36 %	96 ± 6	78 ± 24	72 ± 20	92 ± 6	<0.0001	0.0009	ns
CD36 MFI	1704 ± 234	1170 ± 650	1125 ± 452	834 ± 294	<0.0001	0.01	<0.0001
CD105 %	21 ± 6	23 ± 16	37 ± 30	19 ± 8	ns	ns	ns
CD105 MFI	190 ± 76	208 ± 178	451 ± 670	130 ± 25	ns	ns	0.01
CD71 MFI	3207 ± 1050	2000 ± 1478	1077 ± 1214	1228 ± 1019	0.004	0.006	0.006
CD71 CV	42 ± 9	108 ± 97	140 ± 6	73 ± 13	<0.0001	<0.0001	<0.0001

Abbreviations: MDS, myelodysplastic syndromes; B12 def, vitamin B12 deficiency; PNH, paroxysmal nocturnal hemoglobinuria; FSC, forward light scatter; SSC, sideward light scatter; MFI, mean fluorescence intensity (arbitrary units); %, percentage of positive cells within relative compartment; CV, coefficient of variation; ns, not significant. Data are expressed as mean ± one standard deviation. p1: controls vs MDS; p2: controls vs B12; p3: controls vs PNH.

of 30 patients with newly diagnosed MDS were investigated; according to WHO, they were classified as follows: RA (eight patients); RARS (refractory anemia with ring sideroblasts) (one); RCMD (refractory cytopenia with multilineage dysplasia) (seven); myelodysplastic syndrome-unclassified (one); RAEB-1 (refractory anemia with excess blasts) (nine); and RAEB-2 (four). According to IPSS, they were stratified as follows: low risk, 10 cases; intermediate-1, 9; intermediate-2, 8; high risk, 3.

Phenotypic Analysis of MDS Compared to Controls

The phenotypic parameters of MDS were individually compared to analogue control values (Table 2). As already described by several reports [11–14], one finding emerging from our study concerned precursor B cells, not detectable in the majority (70%) of MDS patients. Furthermore, several alterations emerged in MDS within CD34+ and mature compartments.

Phenotypic Analysis of B12 def Compared to Controls

Some abnormalities within the granulocytic compartment were specifically associated with B12 def: SSC signal was increased compared to controls, as it likely expressed the phenotypic counterpart of hypersegmented cells, often observed morphologically. Erythroid compartment showed several alterations, primarily regarding its relative percentage on global cellularity, which was significantly increased. Furthermore, erythroid cells had higher FSC and SSC, and a trend to a weaker expression of CD36 and CD71 compared to controls.

Phenotypic Analysis of PNH Compared to Controls

The analysis of BM from PNH patients showed some significant deviations. Some of them were linked to lack of GPI, whereas others were not. With respect to CD34+ cells, either their total amount or B lymphoid precursors were reduced; B precursors were undetectable in five out of eight cases. Higher percentages of positivity for CD7 and CD38 were observed on PNH CD34+ cells compared to the normal reference. Within granulocytic compartment, the percentage of CD16-highly positive neutrophils was lower than in controls; this finding is consistent with the GPI-dependent tethering of CD16. No further relevant changes emerged for granulocytic compartment. With regard to monocytic cells, CD14 pattern was obviously influenced by the lack of GPI and resulted significantly lower than in

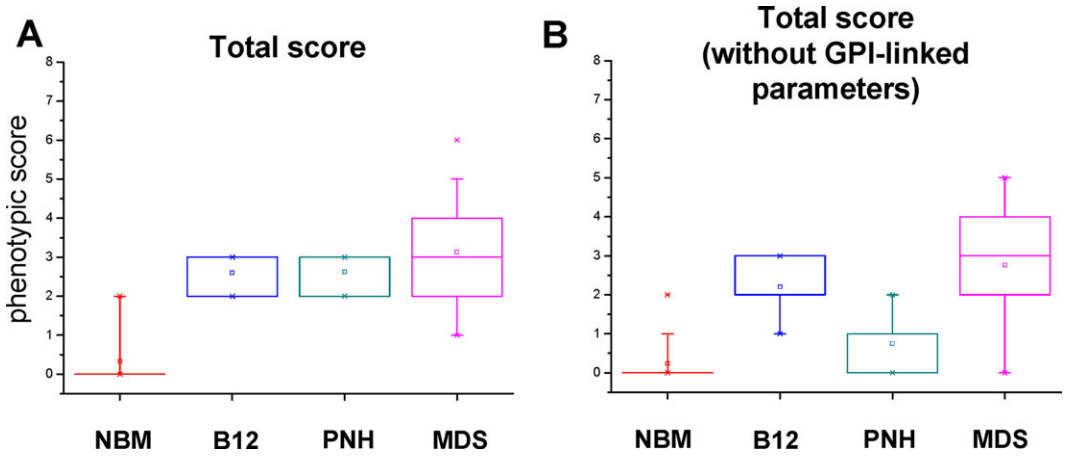

FIG. 2. Multi-parameter analysis of bone marrow samples demonstrates disease-related quantitative abnormalities, appraised by a validated phenotypic score [21]. Box plots were generated by SPSS software. Boxes represent the interquartile range that contains 50% of the subjects, the horizontal line in the box marks the median, the small square inside indicates mean value and bars show the range of values. NBM, normal bone marrow; B12, vitamin B12 deficiency; PNH, paroxysmal nocturnal hemoglobinuria; MDS, myelodysplastic syndromes. [Color figure can be viewed in the online issue which is available at wileyonlinelibrary.com]

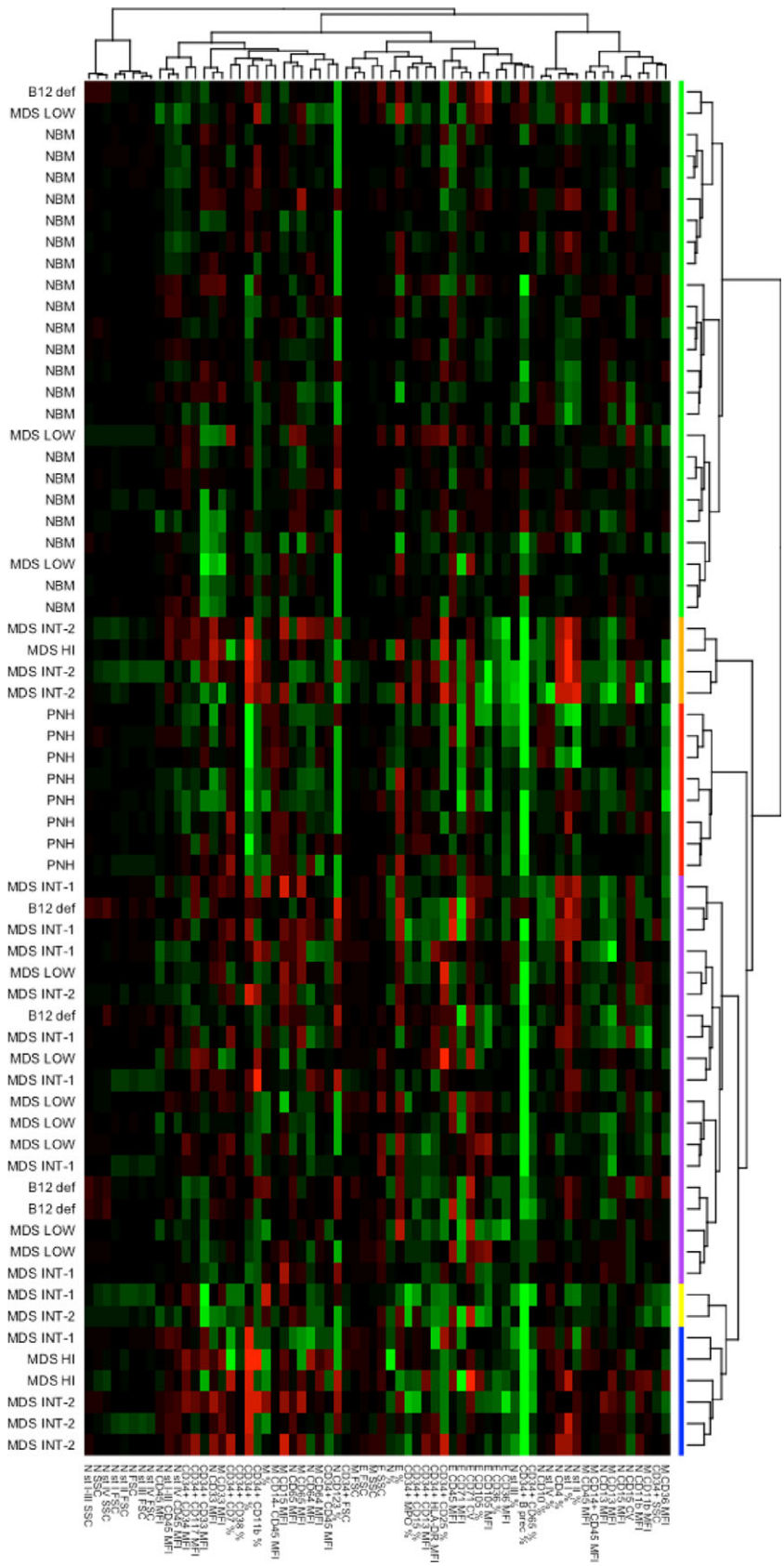

FIG. 3. Cluster analysis of normal bone marrows, PNH, MDS, and vitamin B12 deficiency: PNH cases grouped in a separate cluster due to a distinctive phenotypic profile. Cluster analysis of normal bone marrow (NBM), MDS (each case with relative IPSS score), PNH, and B12 deficiency (B12 def) based on the phenotypic parameters within distinct subsets of BM cell compartments. GPI-related antigens were excluded from this analysis. Rows represent individual BM samples from NBM, MDS, PNH, and B12 def; columns represent the normalized log2 ratios of the percentage of individual cell subsets and the mean fluorescence intensity (MFI; arbitrary relative linear units) obtained for each marker analyzed in a given cell population divided by the mean value obtained for that parameter in all control samples. The value of each parameter is represented in a color code according to control values: red represents expression greater than the mean, green represents expression lower than the mean; color intensity represents the magnitude of the deviation from the mean. [Color figure can be viewed in the online issue which is available at wileyonlinelibrary.com]

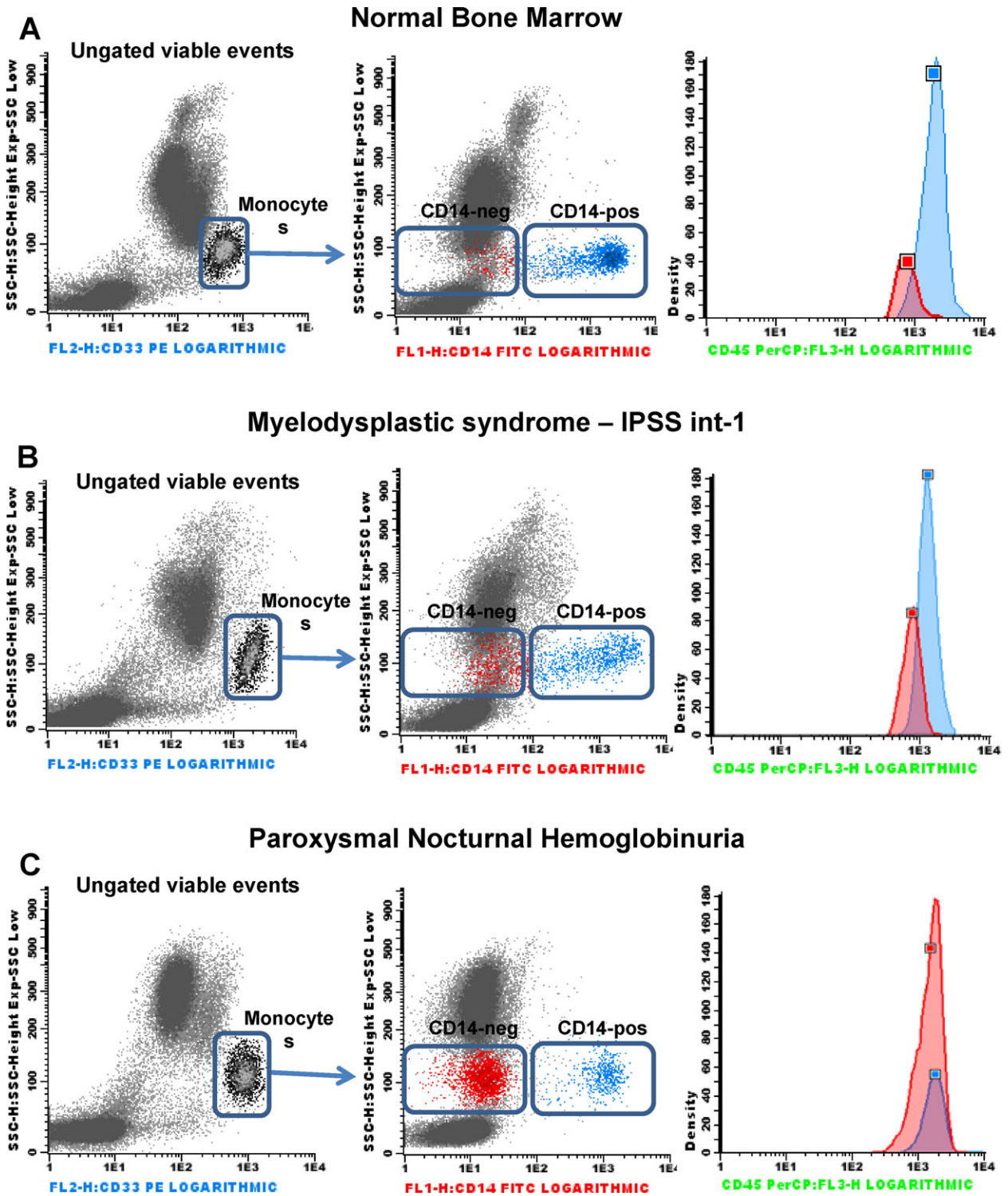

FIG. 4. Distinctive pattern for CD14 and CD45 on monocytes in PNH cases. Histogram plots show the pattern of CD45 on monocytes, gated by CD33 intensity, according to CD14 expression in three illustrative bone marrow samples from controls (panel **A**), MDS (**B**), and PNH (**C**) groups. CD14-negative monocytes in PNH showed significantly higher levels of CD45 relative to their counterparts in normal BM or MDS, which is consistent with the GPI-related lack of CD14 that is independent on maturation stage. Histogram and dot plots were created by using Infinicyt software. [Color figure can be viewed in the online issue which is available at wileyonlinelibrary.com]

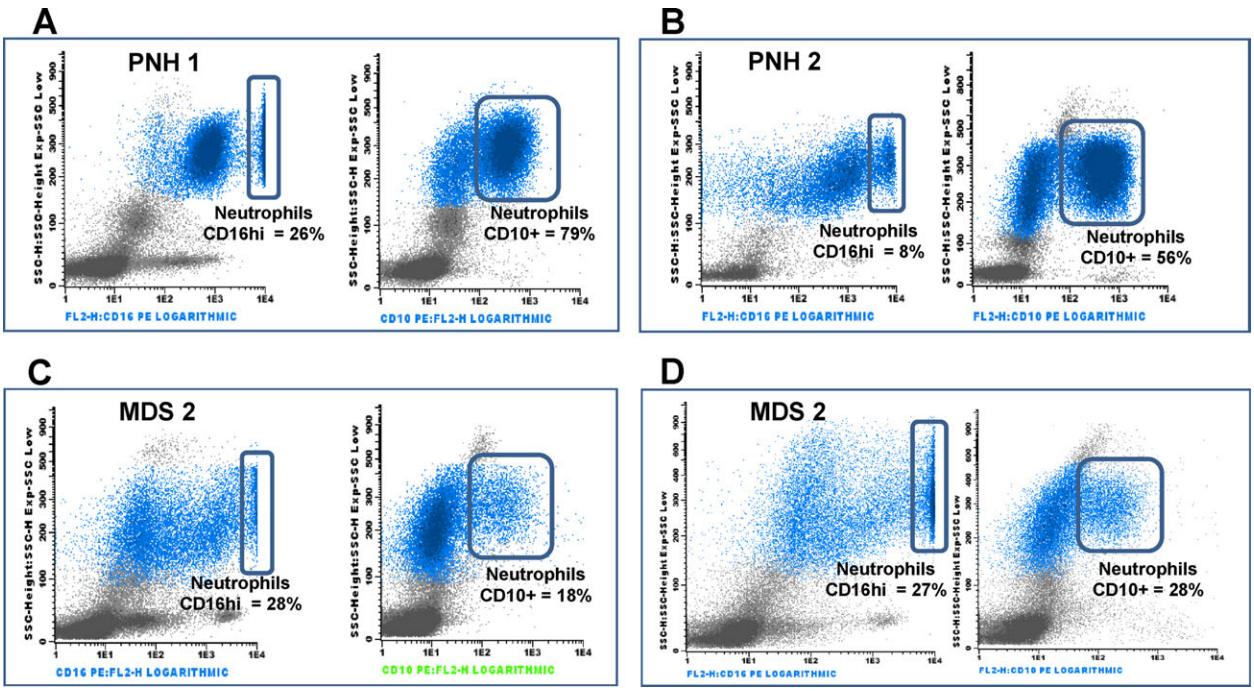

FIG. 5. Distinctive pattern for CD10 and CD16 on granulocytic compartment in PNH cases. Dot plots display the pattern of CD16 and CD10 within the bone marrow granulocytic compartment (blue color; gated on the basis of CD45 reactivity and SSC) in two illustrative cases of PNH (panels **A**–**B**) and MDS (**C**–**D**). MDS show a parallel decrease of CD16hi and CD10+ elements whereas CD10 expression is preserved in PNH. Histogram and dot plots were created by using Infinicyt software. [Color figure can be viewed in the online issue which is available at wileyonlinelibrary.com]

controls. One unexpected finding concerned a GPI-unrelated molecule: CD36 intensity was reduced relative to normal. In five cases, it was possible to address the expression of CD36 according to CD14: CD14-negative and CD14-positive monocytes expressed similar amounts of CD36 (mean MFI 554.44 vs 556.26, ns). Erythroid compartment showed increased SSC, a weaker and more heterogeneous expression of CD71 and an abnormal pattern for CD36. Of note, CD36 was maintained in terms of percentage of positivity, while its expression was globally less intense than on normal counterpart.

Phenotypic Scores in MDS, B12 def, and PNH

In order to estimate the degree of abnormality, we applied a previously described and validated phenotypic score [21] to our cases. The mean scores assigned to PNH and B12 def were generally lower than for MDS (Fig. 2A) but PNH cases had a remarkable overlap with MDS. Since phenotypic score included some GPI-linked antigens, we repeated our analysis after excluding the relative parameters (*i.e.* CD14 percentage on monocytes, CD16 percentage on neutrophil compartment). As we can infer from the resulting plot (Fig. 2B), PNH score continued to be abnormal and overlapping with MDS even when counting out GPI deficiency.

Cluster Analysis: Identification of a Distinctive Phenotypic Profile for PNH

We performed a two-step cluster analysis to verify the capability of the whole phenotypic profile to separate different diseases: i) an unsupervised analysis including all 69 parameters; ii) an analysis excluding GPI-related antigens, to get further insights into abnormalities not dependent on GPI. PNH patients clustered in both analysis (i) (see Supplemental data) and (ii) (Fig. 3). We then revised the results of the clustering analysis, aiming to pinpoint disease-specific patterns. Abnormalities in erythroid compartment were shared by all disease categories. No single erythroid phenotypic abnormality was specifically associated with any disease group; rather, direction and extent of abnormalities appeared independent of the underlying condition. CD36 expression pattern was assessed by both percentage and intensity. The combination of the two parameters was different in PNH, since CD36 was maintained in terms of percentage but less intense. In MDS and B12 def, the percentage and the intensity were both abnormally reduced. Given the potential variability in CD36 MFI, due to the presence of a bi-modal expression, we estimated its value focusing on CD36-positive population: this approach confirmed this antigen to be hypo-expressed in PNH (mean MFI 790.64) compared to normal BM (1781.70; $p<0.0001$). The mere analysis of GPI-linked antigens would have not been sufficient to distinguish PNH from MDS. Indeed the pattern of these antigens in some MDS cases mimic what was observed in PNH. As an example, in our series, 11 of 30 (36.7%) MDS cases displayed a CD14-negative monocytic population equal to or higher than 20% of cells within relative compartment, likely as a consequence of impaired maturation. The parallel trend of CD45 aided to differentiate between MDS and PNH: CD14-negative monocytes in

PNH showed significantly higher levels of CD45 relative to their counterpart in MDS (and even in normal BM) (Fig. 4). Similarly, CD16-highly positive granulocytic cells were frequently reduced in MDS (48% of cases) compared to controls; in these cases, we observed a parallel decrease of CD10 expression that was maintained in PNH instead (Fig. 5). Clustering of PNH cases was essentially provided by the simultaneous assessment of the whole phenotypic profile, rather than by single abnormalities. The very fact that PNH cases clustered together, even after removing GPI-related parameters, confirmed further that PNH shows a distinctive phenotypic profile exceeding GPI-dependent antigens.

DISCUSSION

MDS and PNH have remarkable overlapping areas, ranging from pathogenesis to clinical picture. PNH clones can be detected in the setting of MDS, and their presence may not be related to the pre-leukemic nature of MDS but rather linked to BM failure, similar to aplastic anemia [22]. Furthermore, PNH can represent the clinical evolution of another BM disorder, and especially of MDS cases.

Due to clinical and morphological similarities, the distinction between MDS and PNH can sometimes be difficult. We have analyzed systematically flow cytometry (FC) data resulting from the study of BM cells from patients with MDS and PNH. In the latter disease, the observed phenotypic changes were beyond the expected GPI-related abnormalities. The total amount of CD34+ cells on global cellularity was reduced. This finding has already been reported [23] and is not surprising taking into consideration the autoimmune-mediated attack that provides a relative advantage to PNH clone [24]. The proportions among CD34+ subpopulations were also affected: B lymphoid precursors were not detectable in the majority of our cases and the mean percentage of CD34+/CD38+ fraction was higher than in normal BM. The latter finding is consistent with the reduced frequency of the most immature CD34+/CD38− subpopulation, about which Elebute et al. have previously reported, suggesting a stem cell defect in the pathogenesis of PNH [25]. The antigenic profile of CD34+ cells did not show relevant abnormalities; the increased expression of CD7 was probably related to B precursors reduction, since CD7 is normally expressed by a fraction of myeloid CD34+ cells. These data parallel the lack of significant differences in gene expression profiles between CD34+ cells from PNH patients and healthy individuals described by Chen et al. [26]. As for morphology, several abnormalities on maturing cell compartments emerged. Our systematic approach combining all parameters allowed us to overcome the overlap with MDS that was described by morphology. Specifically, the simultaneous assessment of some phenotypic marks was distinctive for PNH. The trend of expression of CD45 and CD10, if analyzed in parallel with GPI-linked antigens, allowed to work out phenotypic changes as being associated with MDS rather than PNH. CD14 and CD16 are acquired within respective lineage at the final stages of maturation. In normal BM, a relevant fraction of cells are physiologically negative for these antigens, and in MDS, these fractions quite often increase, most likely as a result of impaired maturation. The parallel pattern of CD14 and CD45 on monocytes aided in distinguishing between MDS and PNH, since CD45 increases along with monocytic maturation. CD14-negative monocytes in PNH showed significantly higher levels of CD45 relative to their counterparts in MDS, which is coherent with the GPI-related lack of CD14, mainly independent on maturation stage (Fig. 4). Analogue mechanism accounted for the dissociation between CD10 and CD16 in the granulocytic compartment in PNH compared to MDS (Fig. 5).

The careful assessment of these parameter combinations can be very useful in the diagnostic process of cytopenia, especially when FC analysis is not driven toward PNH by a specific clinical query, and furthermore because some MDS-related abnormalities concern GPI-linked molecules. In this respect, it is important not to miss PNH in a patient thought to have MDS, primarily because of the high risk of thrombosis associated with the former disease. Furthermore, some phenotypic changes emerging from our data might be related to PNH physiopathology. Monocytic and erythroid compartments appeared to express lower levels of CD36 compared to controls. It was interesting to observe that erythroid lineage in MDS and B12 def shared similar patterns of CD36 abnormality (*i.e.* decreased percentage of CD36-positive cells), reasonably attributed to ineffective erythropoiesis. On the contrary, PNH showed CD36 hypo-expression with normal percentage, probably due to a different mechanism. As the hypo-expression of CD36 on monocytic cells did not depend on belonging to PNH clone, it could be related to external factors influencing the expression on both normal residual and PNH cells. CD36 is a glycoprotein belonging to the scavenger receptor type B family and is expressed in a variety of cells and tissues [27]. CD36 and CD36-related pathways have been involved in the pathogenesis of atherosclerosis and thrombosis [27]. Some published evidence suggests that a reduction in CD36 expression on monocytes might be responsible of a thrombophilic state. First, CD36 is involved in the release of arachidonic acid from cell membranes and thus contributes to the generation of proinflammatory eicosanoids. Monocytic cells null for CD36 have been reported to produce paradoxically more prostaglandin E2, probably as a result of compensatory up-regulation of cyclooxygenase [28]. Furthermore, the release of pro-coagulant phospholipid micro-particles from PNH erythrocytes by complement activation has been proposed as a mechanism of PNH-related thrombophilia [29]. Given the role of CD36 in scavenging of cell-derived micro-particles, one might surmise a reduction of this process due to the molecule hypo-expression. As such, our data deserve further investigation in order to get an insight into the potential participation to the well-established PNH-related thrombophilic state [30].

In conclusion, this study allowed us to investigate systematically the phenotypic profile of BM cells from patients with PNH; our data provided useful antigenic patterns to distinguish between PNH and MDS. Besides, some PNH-related phenotypic changes might be involved in the physiopathology of the disease and further studies addressing this issue are warranted.

ACKNOWLEDGMENTS

This study was supported by Istituto Toscano Tumori, Ente Cassa di Risparmio di Firenze, and Regione Toscana.

LITERATURE CITED

1. Takeda J, Miyata T, Kawagoe K, Iida Y, Endo Y, Fujita T, Takahashi M, Kitani T, Kinoshita T. Deficiency of the GPI anchor caused by a somatic mutation of the PIG-A gene in paroxysmal nocturnal hemoglobinuria. Cell 1993;73:703–711.
2. Bessler M, Mason PJ, Hillmen P, Miyata T, Yamada N, Takeda J, Luzzatto L, Kinoshita T. Paroxysmal nocturnal haemoglobinuria (PNH) is caused by somatic mutations in the PIG-A gene. EMBO J 1994;13:110–117.
3. Nicholson-Weller A, March JP, Rosenfeld SI, Austen KF. Affected erythrocytes of patients with paroxysmal nocturnal hemoglobinuria are deficient in the complement regulatory protein, decay accelerating factor. PNAS 1983;80:5066–5070.
4. Davitz MA, Low MG, Nussenzweig V. Release of decay-accelerating factor (DAF) from the cell membrane by phosphatidylinositol-specific phospholipase C (PIPLC). Selective modification of a complement regulatory protein. J Exp Med 1986;163:1150–1161.
5. Rosse WF, Ware RE. The molecular basis of paroxysmal nocturnal hemoglobinuria. Blood 1995;86:3277–3286.
6. Parker C, Omine M, Richards S, Nishimura J, Bessler M, Ware R, Hillmen P, Luzzatto L, Young N, Kinoshita T, et al. Diagnosis and management of paroxysmal nocturnal hemoglobinuria. Blood 2005;106:3699–3709.
7. Vardiman JW, Thiele J, Arber DA, Brunning RD, Borowitz MJ, Porwit A, Harris NL, Le Beau MM, Hellström-Lindberg E, Tefferi A, et al. The 2008 revision of the World Health Organization (WHO) classification of myeloid neoplasms and acute leukemia: rationale and important changes. Blood 2009;114:937–951.
8. Araten DJ, Swirsky D, Karadimitris A, Notaro R, Nafa K, Bessler M, Thaler HT, Castro-Malaspina H, Childs BH, Boulad F, et al. Cytogenetic and morphological abnormalities in paroxysmal nocturnal haemoglobinuria. Br J Haematol 2001;115:360–368.
9. Borowitz MJ, Craig FE, DiGiuseppe JA, Illingworth AJ, Rosse W, Sutherland DR, Wittwer CT, Richards SJ. Guidelines for the diagnosis and monitoring of paroxysmal nocturnal hemoglobinuria and related disorders by flow cytometry. Cytometry Part B 2010;78B:211–230.
10. Sutherland DR, Keeney M, Illingworth A. Practical guidelines for the high-sensitivity detection and monitoring of paroxysmal nocturnal hemoglobinuria clones by flow cytometry. Cytometry Part B 2012;82B:195–208.
11. Ogata K, Nakamura K, Yokose N, Tamura H, Tachibana M, Taniguchi O, Iwakiri R, Hayashi T, Sakamaki H, Murai Y, et al. Clinical significance of phenotypic features of blasts in patients with myelodysplastic syndrome. Blood 2002;100:3887–3896.
12. Kussick SJ, Fromm JR, Rossini A, Li Y, Chang A, Norwood TH, Wood BL. Four-color flow cytometry shows strong concordance with bone marrow morphology and cytogenetics in the evaluation for myelodysplasia. Am J Clin Pathol 2005;124:170–181.
13. Matarraz S, Lopez A, Barrena S, Fernandez C, Jensen E, Flores J, Barcena P, Rasillo A, Sayagues JM, Sanchez ML, et al. The immunophenotype of different immature, myeloid and B-cell lineage-committed CD34+ hematopoietic cells allows discrimination between normal/reactive and myelodysplastic syndrome precursors. Leukemia 2008;22:1175–1183.
14. van de Loosdrecht AA, Alhan C, Béné MC, Della Porta MG, Dräger AM, Font P, Germing U, Haase D, Homburg CH, Ireland R, et al. Standardization of flow cytometry in myelodysplastic syndromes: report from the first European Leukemia Net working conference on flow cytometry in myelodysplastic syndromes. Haematologica 2009;94:1124–1134.
15. Della Porta MG, Lanza F, Del Vecchio L. Flow cytometry immunophenotyping for the evaluation of bone marrow dysplasia. Cytometry Part B 2011;80B:201–211.
16. Mitelman FP. An International System for Human Cytogenetic Nomenclature. Basel: S. Karger; 1995.
17. Greenberg P, Cox C, LeBeau MM, Fenaux P, Morel P, Sanz G, Sanz M, Vallespi T, Hamblin T, Oscier D, et al. International scoring system for evaluating prognosis in myelodysplastic syndromes. Blood 1997;89:2079–2088.
18. Owens M, Vall HG, Hurley AA, Wormsley SB. Validation and quality control of immunophenotyping in clinical flow cytometry. J Immunol Met 2000;243:33–50.
19. Kraan J, Gratama JW, Keeney M, D'Hautcourt JL. Setting up and calibration of a flow cytometer for multicolor immunophenotyping. J Biol Regul Homeost Agents 2003;17:223–233.
20. Bieliauskas S, Fine N, Douglas-Nikitin V, Blenc AM. Paroxysmal nocturnal hemoglobinuria clones are not present in HIV positive patients. Cytometry Part B 2010;80B:64–67.
21. Wells DA, Benesch M, Loken MR, Vallejo C, Myerson D, Leisenring WM, Deeg HJ. Myeloid and monocytic dyspoiesis as determined by flow cytometric scoring in myelodysplastic syndrome correlates with the IPSS and with outcome after hematopoietic stem cell transplantation. Blood 2003;102:394–403.
22. Wang SA, Pozdnyakova O, Jorgensen JL, Medeiros LJ, Stachurski D, Anderson M, Raza A, Woda BA. Detection of paroxysmal nocturnal hemoglobinuria clones in patients with myelodysplastic syndromes and related bone marrow diseases, with emphasis on diagnostic pitfalls and caveats. Haematologica 2009;94(1):29–37.
23. Maciejewski JP, Sloand EM, Sato T, Anderson S, Young NS. Impaired hematopoiesis in paroxysmal nocturnal hemoglobinuria/aplastic anemia is not associated with a selective proliferative defect in the glycosylphosphatidylinositol-anchored protein-deficient clone. Blood 1997;89:1173–1181.
24. Karadimitris A, Luzzatto L. The cellular pathogenesis of paroxysmal nocturnal haemoglobinuria. Leukemia 2001;15:1148–1152.
25. Elebute MO, Rizzo S, Tooze JA, Marsh JCW, Gordon-Smith EC, Gibson FM. Evaluation of the haemopoietic reservoir in de novo haemolytic paroxysmal nocturnal haemoglobinuria. Br J Haematol 2003;123:552–560.
26. Chen G, Zeng W, Maciejewski JP, Kcyvanfar K, Billings EM, Young NS. Differential gene expression in hematopoietic progenitors from paroxysmal nocturnal hemoglobinuria patients reveals an apoptosis/immune response in 'normal' phenotype cells. Leukemia 2005;19:862–868.
27. Silverstein RL, Li W, Park YM, Rahaman SO. Mechanisms of cell signaling by the scavenger receptor CD36: implications in atherosclerosis and thrombosis. Trans Am Clin Climatol Assoc 2010;121:206–220.
28. Kuda O, Jenkins CM, Skinner JR, Moon SH, Su X, Gross RW, Abumrad NA. CD36 is involved in store operated calcium flux, phospholipase A2 activation and production of prostaglandin E2. J Biol Chem 2011;286:17785–17795.
29. Kozuma Y, Sawahata Y, Takei Y, Chiba S, Ninomiyaet H. Procoagulant properties of microparticles released from red blood cells in paroxysmal nocturnal haemoglobinuria. Br J Haematol 2011;152:631–639.
30. Luzzatto L, Gianfaldoni G, Notaro R. Management of paroxysmal nocturnal haemoglobinuria: a personal view. Br J Haematol 2011;153:709–720.